Microstructural characterization and simulation of damage for geared sheet components

IOP Conf. Series: Journal of Physics: Conf. Series **896** (2017) 012076 doi:10.1088/1742-6596/896/1/012076

Microstructural characterization and simulation of damage for geared sheet components

G Gerstein[1], K Isik[2], F Gutknecht[2], P Sieczkarek[2], J Ewert[1], A E Tekkaya[2], T Clausmeyer[2] and F Nürnberger[1]

[1] Institut für Werkstoffkunde (Materials Science), Leibniz Universität Hannover, Germany, e-mail: gerstein@iw.uni-hannover.de
[2] Institute of Forming Technology and Lightweight Components (IUL), TU Dortmund University, Germany

Abstract. The evolution of damage in geared components manufactured from steel sheets was investigated, to analyse the influence of damage caused by the sheet-bulk-metal forming. Due to the inhomogeneous and multi-axial deformation in the investigated parts, different aspects such as the location-dependent shape and size of voids are analysed by means of various microscopic methods. In particular, a method to characterize the state of damage evolution, i. e. void nucleation, growth and coalescence using scanning electron microscopy (SEM) is applied. The investigations reveal a strong dependence of the void area fraction, shape of voids and thus damage evolution on the loading mode. The microstructural analysis is complemented with FEM simulations using material models which consider the characteristics of the void evolution.

Keywords: Sheet-bulk metal forming; Sheet metal; Damage; Microstructure; Voids; Load path dependence; Microscopy; Simulation

1. Introduction

In sheet-bulk-metal forming (SBMF) processes material is redistributed in the direction perpendicular to the sheet thickness to create functional elements such as geared components [1]. The manufacturing process involves the combination of both drawing and indentation operations. These result in a combination of tensile and compressive loads during forming. The desired plastic deformation is accompanied by the evolution of voids. In dual phase steels the voids nucleate and grow mainly inside the martensite particles or along the ferrite/martensite interfaces [2]. Landron et al. have shown that for the dual phase steel void coalescence occurs just before final fracture and in particular local coalescence occurs between neighbouring cavities [3]. Similarly, Avramovic-Cingara et al. [4] considered only the mechanisms of nucleation and growth of voids.

Previous work by Landron et al. [5] and others have used X-Ray microtomography to investigate void events in the microstructure. Such systems make it possible to obtain 3D information of macroscopic fields. Usually, this approach has a spatial resolution of 2 µm or more likely in this context a voxel size of 1.6 µm³. This is very helpful for in-situ observations of void events. Especially concerning void coalescence. However, when to differentiate whether a void has newly nucleated or grown this approach has some uncertainties. Measurement of void shape and size using the special polishing method presented in the following allows observing voids at the nano scale (Figure 1). The corresponding voxel size of this approach is 8 nm³. While the studies using microtomography are given for the micro level, this approach looks at the nanoscale. Nevertheless, the data of both are in very good correlation.

Such defects result in a reduction of the load bearing capacity of metallic parts. When the void size reaches a critical level, either by growth or coalescence, the formation of cracks leads to macroscopic failure [6]. According to Lemaitre [7] the scalar damage variable D is determined by the ratio of the Young's modulus with defects to its value in a defectless condition. This damage variable D can be understood as the ratio of the area of the defects like microvoids, or microcracks to the total area (assuming no damage) of a considered material point. Similarly, for the damage models of the Gurson family, a scalar void volume fraction f is directly correlated to the damage of the material [8]. In this

case f denotes the ratio of void volume to total volume of the considered material point. The evolution of voids during forming of parts, especially by SBMF has not yet been analysed comprehensively. Previous investigations of the authors for a geared component manufactured by SBMF revealed that under compressive stress states, the void volume fraction (and thus the damage) may decrease [9].

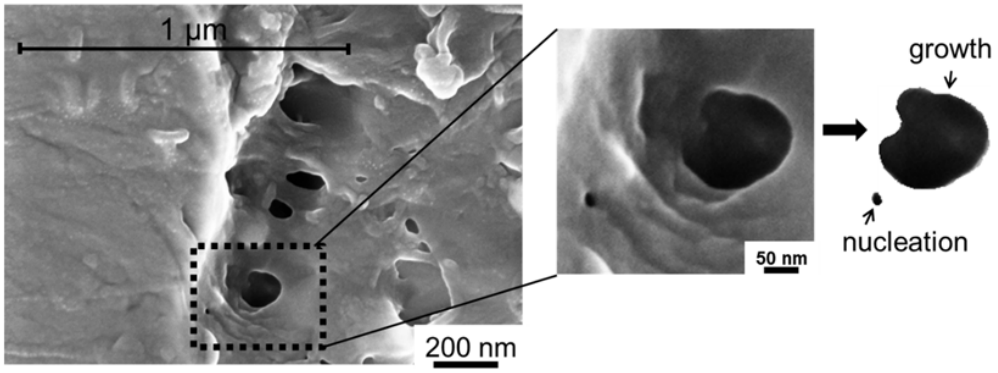

Figure 1. Micrograph of typical dimensions.

For a detailed analysis of the damage evolution during SBMF a simplified specimen has been developed. Thus, different levels of pre-strain and subsequent forming can be combined to investigate the influence of load path changes on the evolution of damage and fracture. The experimental setup of this simplified specimen is given in section 2. Section 3 presents the sample preparation for the microstructural analysis with both light microscopy and scanning electron microscopy (SEM) of the tested specimen. Details about the simulation of the experiment with respect to damage and failure are given in section 4. The results of the simulations are compared to those of the microstructural analysis in section 5.

2. Experimental setup

The forming experiments were carried out on a five-axis forming press that was specially designed for the demands of incremental sheet-bulk metal forming processes [10]. An important feature is the availability of several axes of motion. The used setup enables a simultaneous conduction of different operations, such as tensile and compressive processes [11]. In order to conduct experiments which allow the analysis of a combined tensile and compression deformation and thus to investigate the strain path dependency of the material due to a multi-axial deformation, the experiments were run in a consecutive sequence. After an initial tensile preforming to specific elongation ratios, an indentation step was conducted with different indentation depths (cf. **Table *1***).

Table 1. Process parameters

Tensile strain	Indentation depth	Result
10%	3.3 mm	OK
10%	3.8 mm	Crack
15%	2.8 mm	OK
15%	3.3 mm	Crack

The sheet geometry was designed in accordance with conventional tensile tests to achieve uniform deformation in the centre region and realize plane stress conditions during pure tensile loading. Figure 2 presents the used setup, workpiece and the tool geometries. The specimens were manufactured by laser cutting from the dual phase steel DP600 (WN 1.0936) with an initial thickness of s_0 = 2 mm. The experiments were performed without lubricants at room temperature with a constant indentation velocity

of v = 1 mm/s. The indenter was manufactured from a powder metallurgy high-speed steel ASP®2023 (WN 1.3344) and vacuum hardened to a surface hardness of 60 HRC. All other components of the setup were made of S 235 JR (WN 1.0038) steel plates containing screws for a defined clamping and positioning of the specimen.

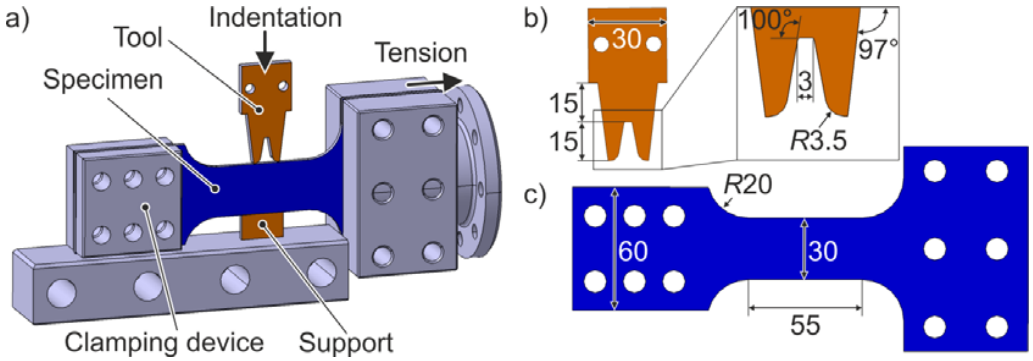

Figure 2. a) Experimental setup (schematic), b) Tool geometry, c) Workpiece geometry.

3. Microstructural Analysis

Following the experiments the specimen were cut into pieces. Figure 3 displays the zones from which samples have been prepared for micrographic analysis. Due to anisotropy of both material and loading path, micrographs of cross sectional cuts (P1-P4, PTC), as well as longitudinal cuts (PT, P5, P6) have been prepared. PT has been subjected to only tensile loading, while PTC was subjected to additional compression. P1 – P6 have in common a fully three-dimensional stress state, which is representative for complex forming operations. The preparation followed the method presented in [12]. Special emphasis is given to the final polish for one hour in a vibratory polisher. The samples from each zone have been analysed with 5000x magnification. At each zone a grid of 5x5 images covered an area of 9775 µm². Back scattered electrons (BSE) were used as primary signal source.

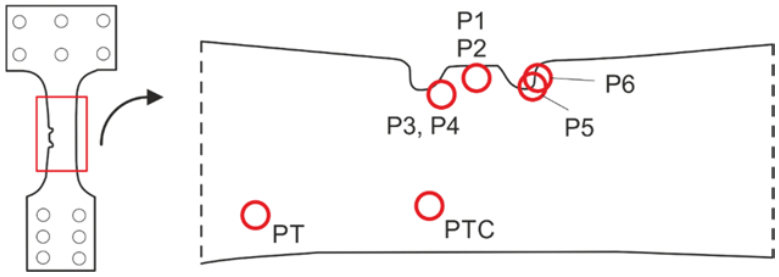

Figure 3. Localization of investigated zones on the specimen.

4. Simulation setup

Gurson's porous plasticity model [8] is used to predict the evolution of void events and fracture. The applied model includes the enhancement introduced in [13] to model the accelerated increase in the void content due to coalescence and the model extension introduced in [14] to include the void growth under shear stress states. The model was implemented in Abaqus as a user defined subroutine VUMAT. A detailed description is given in [15]. The process was simulated using 8-noded C3D8R (8-node linear brick, reduced integration with hourglass control) elements in Abaqus/Explicit. The mesh size at the deformation zone is 0.25 mm, which is reasonable for the smallest indenter tip radius of 0.5 mm. In order to eliminate the problem of excessive element distortion due to large deformations at the forming zone, an Arbitrary-Lagrangian-Eulerian (ALE) meshing scheme is applied. The crack is represented by

the deletion of those elements, for which the void volume fraction reaches the critical value f_f. The indenter is modelled as a rigid body.

Table 2. Material properties (DP600, sheet thickness 2 mm)

Elastoplastic properties	Modulus of Elasticity in MPa	Poisson's ratio	Yield strength in MPa	Lankford's coefficients			Swift hardening: $\sigma_y[e^p]=K(e_0+e^p)^n$		
				r_0	r_{45}	r_{90}	K in MPa	e_0	n
	201400	0.3	359	0.974	0.972	1.217	983	0.00232	0.19

Gurson Model Parameters	f_0	q_1	q_2	q_3	f_N	s_N	$e^p{}_N$	f_c	f_f
	0.0008	1.5	1.0	2.25	0.00062	0.1283	0.5421	0.015	0.07

The elastoplastic material properties and the Gurson model parameters for the selected material DP600 sheet (2 mm thickness) are listed in Table 2. The methodology used for the parameter identification is presented in [12]. The model parameters related to void nucleation, growth and coalescence and initial void content are obtained from the micromechanical measurements. The model parameter related to the void growth under shear is obtained by an inversed parameter identification methodology, which utilizes tests such as tensile tests and shear cutting. Mesh size dependency of the model is controlled by this model parameter, which has different values depending on the discretization. The simulation includes two steps as in the process, which are tension of the specimen and indentation of the indenter. The indentation takes place after the removal of the tensile loading on the specimen.

5. Results and Discussion

5.1. Simulation results

Numerical investigation is conducted for the case with initial tensile loading of 10%. For tensile load the designed specimen geometry provides a homogenous plastic strain under the indenter. During indentation a local deformation takes place around the indentation zone. The material under the indenter pushes the neighbouring zones out of the sheet plane (Figure 4). The out of plane component of the strain tensor (ε_{zz}) is maximum under the indenter, such that the material flow out of the sheet plane reaches its maximum and reduces towards the sheet plane.

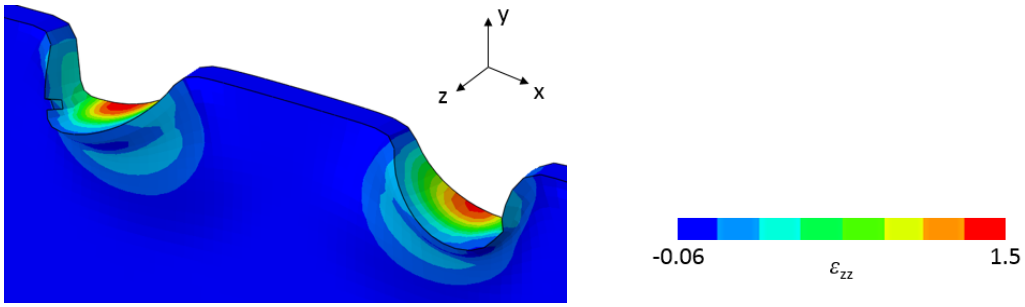

Figure 4. Out of plane component of the strain tensor (distribution) around the indenter at the indentation of 3 mm after 10% tensile loading.

The equivalent plastic strain distribution indicates also locally high strains at the bulging zones, which moves out of the sheet plane. This is also the critical region, where the crack initiates (Figure 5).

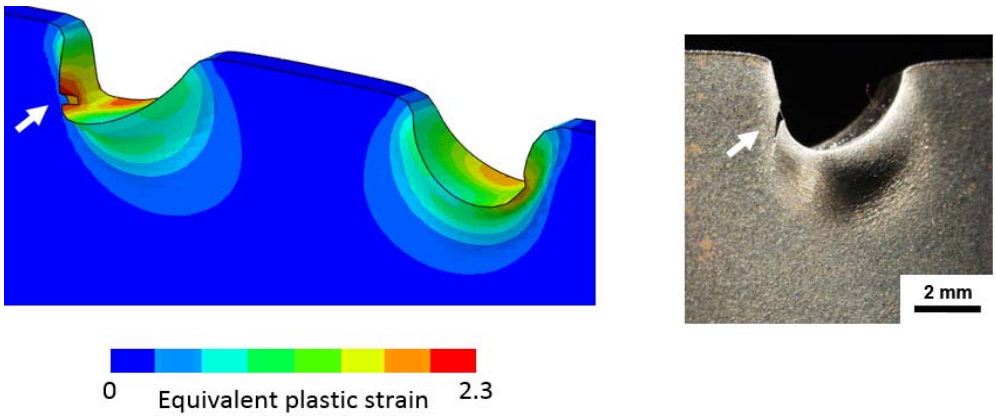

Figure 5. Incipient cracking for the simulation at the indentation of 3 mm and for the experiment at 3.8 mm indentation.

In experimental testing the crack geometry can be analysed only after the punch is released. Therefore, the exact onset of cracking cannot be determined. For 3.3 mm indentation the specimen had no visible crack, while at 3.8 mm a crack was detected. In contrast in simulations the crack initiates at 3.0 mm indentation. Especially for the processes with very local and high deformations, numerical effects such as the effect of the selected mesh size on localization pattern can result in such slight deviations between simulations and experiments. Further mesh studies should be conducted for understanding this effect to improve the predictive performance. Mainly, the simulations are carried out to understand the deformation behaviour before and during the indentation process.

For the following investigation of the void development Figure 6 provides supporting information from the simulation (without ALE) about the load history and the effect on voidage for two representative points. According to Figure 3 and Figure 4, P4 is a point under the indenter where the out of plane strain component has a maximum. P5 is the point on the surface of the specimen which will be deleted first and where the crack initiates.

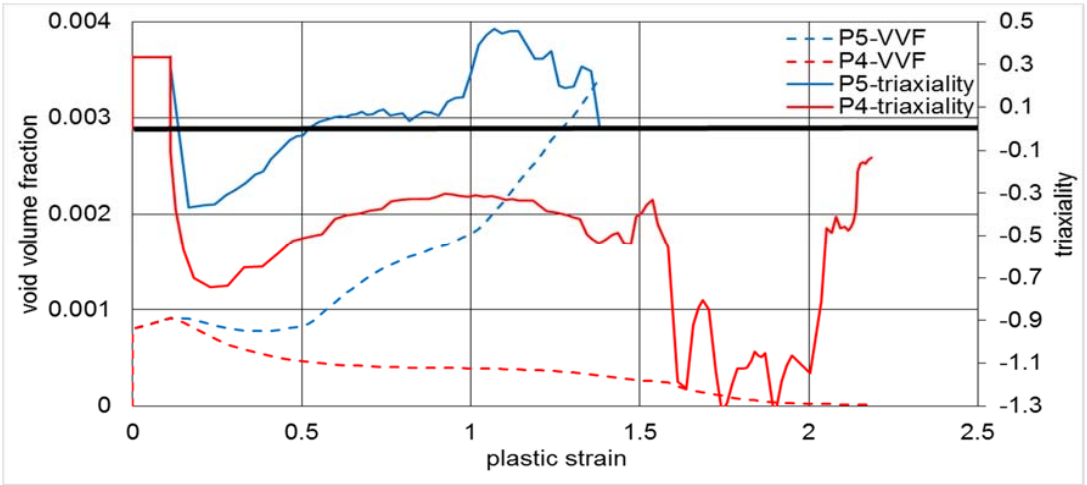

Figure 6. Evolution of void volume fraction (VVF) and triaxiality over plastic strain. The bold horizontal line marks triaxiality of 0.

5.2. Microstructure Analysis

In order to investigate the void development until crack occurrence, the void content in different regions of the specimen were investigated. Figure 7 depicts the counted number of voids at different locations and orientations. Overall, the number of voids is between 125 and 425 for the cross-section view. While

in the upper part of the formed geometry (bridge: P1, P2) no significant increase is present, the number of voids multiplies by almost 4 at the bottom of the indented notches (P3, P4). Areas with homogenous deformation in the thickness direction feature a lot fewer voids than the areas under the indentation. At the bridge and in the point of plane stress (PS) the number of voids only slightly increases. For the longitudinal-section view the number of voids is between 75 and 180. Interestingly, the deformed areas have a reduced number of voids compared to the reference state. Only P6 at the wall of the indentation shows an increased number of voids.

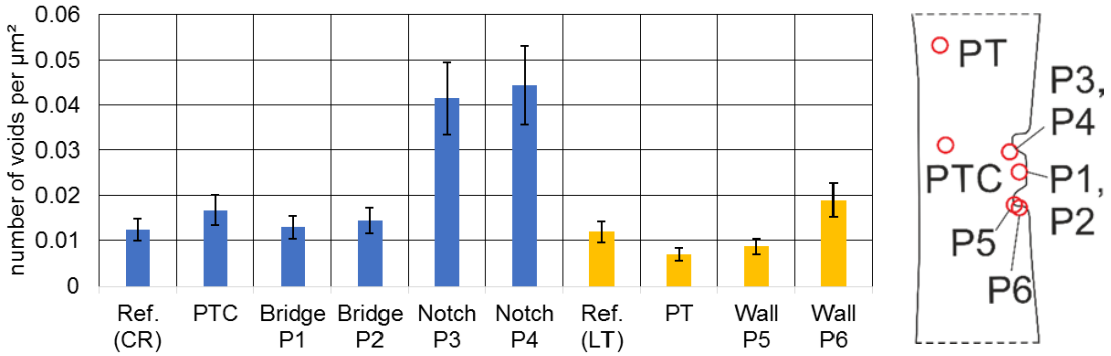

Figure 7. Number of voids at given location in cross-section (CR) view (blue) and longitudinal-section (LT) view (yellow).

The void volume fraction (Figure 8) is calculated as the ratio of void area to total area investigated. For both the cross-sectional and the longitudinal-section view the void volume fraction is highest in areas with severe thickness change. Although the previous analysis has shown that in certain circumstances the number of voids decreases, the void volume fraction for those also increase. In previous research an increase of the mean size of voids was observed [12]. The study focused on the analysis of a notched tensile specimen and an ion slope polishing method. However, the total void volume fraction remained constant. This is a strong indicator for the presence of void coalescence, since the number of voids decreases as opposed to an increase of their individual sizes. This is supported by the fact that P5 is the point of crack initiation. Figure 6 also shows a sudden increase in triaxiality and void volume fraction for the last third of plastic deformation at point P5.

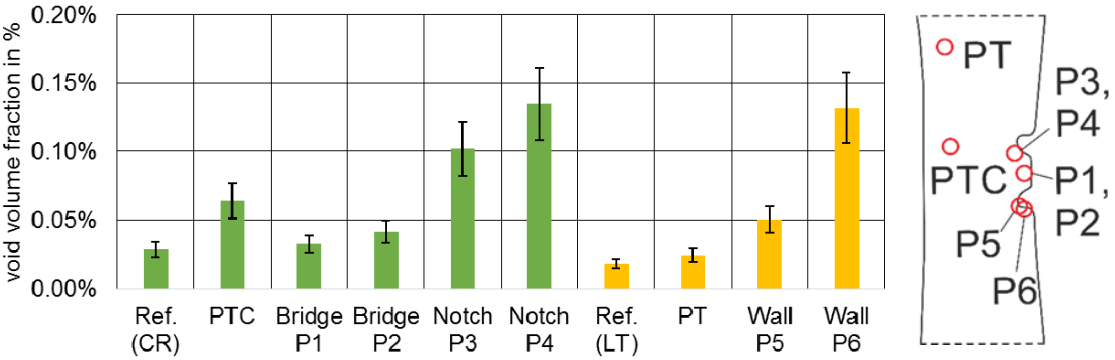

Figure 8. Void volume fraction at given location in cross-section (CR) view (green) and longitudinal-section (LT) view (yellow).

The mean void size is determined as the ratio of total void area to number of voids. For the cross-sectional view, the mean void size is between 0.02 µm² and 0.03 µm² with a peak value of almost 0.04 µm² for plane stress loading (Figure 9). Compared to the longitudinal cut the mean void size is

almost constant. In contrast, the mean void size for the longitudinal cut is changing significantly. The results are of special interest, when looking at the zones P3 and P4. Together with the previous results for both zones another strong hint for the active void mechanism is given. The severely increasing number of voids and volume fraction at almost initial mean void size indicate a numerous nucleation of new voids.

Unfortunately, the simulation is not capable of capturing these effects (Figure 6). In the simulation the void volume fraction of P4 decreases monotonically at indentation. This is coherent to the evolution of triaxiality, which has only negative values during indentation.

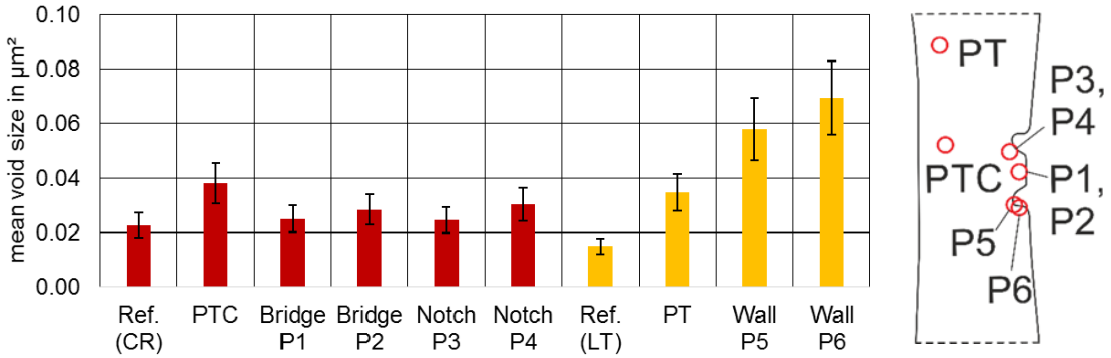

Figure 9. Mean void size at given location in cross-section (CR) view (red) and longitudinal-section (LT) view (yellow).

6. Conclusion

In this study, the void evolution during a successive tension and indentation experiment has been presented. This test mimics a process case with sequentially applied tensile and compressive loadings to a sheet as in a real manufacturing process, such as the process chain of deep drawing and upsetting [9]. With this setup, it is possible to assess onset of fracture and void development until fracture, which does not occur during the mentioned process chain. Sequential application of tensile loading and compression provides the control of the level of pre-strain before indentation.

The simulations show a homogenous plastic deformation zone during tensile loading under the indenter. A slight increase in the voidage can be observed in this stage, depending on the plastic strain that the material point reaches. During the indentation, the localized deformation and the material flow under the indenter can be seen from the simulation results. The material under the indenter pushes the material through the out of sheet plane. As the indentation increases, there is a high localized deformation at the material out of sheet plane. The location of the crack, which occurs at this material protrusion, is captured by the Gurson model correctly with a slight deviation at the critical indentation depth. However, this observation may not be over interpreted in the sense that for all cases, the model parameter f_c coincides with the experimentally determined maximum value.

The microstructural analysis substantiated that the location of crack initiation is subject to some void coalescence before ultimate failure. Furthermore, the analysis has revealed that probably all void evolution mechanisms of nucleation, growth and coalescence are involved during the experiments though not necessarily simultaneously or subsequently. Instead it can be assumed, that under compressive deformation void nucleation dominates, while under tension void coalescence is the primary mechanism. The most critical region at the wall of indent (P6) has a void volume fraction of 0.13%, which is much smaller than the void volume fraction of 7% obtained in [12]. It is expected that the void content increases with an accelerated void coalescence as approaching the outer contour of the material protrusion. However, this hypothesis must be proved with further investigations.

Acknowledgements
The authors gratefully acknowledge funding by the German Research Foundation (DFG) within the scope of the Transregional Collaborative Research Centre on sheet-bulk metal forming (SFB/TR 73) in the project C4 'Analysis of load history dependent evolution of damage and microstructure for the numerical design of sheet-bulk metal forming processes' and the project A4 'Fundamental research and process development for the manufacturing of load-optimized parts by incremental sheet-bulk metal forming'.

References

[1] Merklein M, Allwood JM, Behrens BA, Brosius A, Hagenah H, Kuzman K, et al. Bulk forming of sheet metal. *CIRP Annals - Manufacturing Technology*. 2012;**61**(2):725-45.
[2] Avramovic-Cingara G, Ososkov Y, Jain MK, Wilkinson DS. Effect of martensite distribution on damage behaviour in DP600 dual phase steels. *Mat Sci Eng a-Struct*. 2009;**516**(1-2):7-16.
[3] Landron C, Bouaziz O, Maire E, Adrien J. Experimental investigation of void coalescence in a dual phase steel using X-ray tomography. *Acta Materialia*. 2013;**61**(18):6821-9.
[4] Avramovic-Cingara G, Saleh CAR, Jain MK, Wilkinson DS. Void Nucleation and Growth in Dual-Phase Steel 600 during Uniaxial Tensile Testing. *Metall Mater Trans A*. 2009;**40a**(13):3117-27.
[5] Landron C, Maire E, Bouaziz O, Adrien J, Lecarme L, Bareggi A. Validation of void growth models using X-ray microtomography characterization of damage in dual phase steels. *Acta Materialia*. 2011;**59**(20):7564-73.
[6] Tasan CC, Hoefnagels JPM, ten Horn CHLJ, Geers MGD. Experimental analysis of strain path dependent ductile damage mechanics and forming limits. *Mechanics of Materials*. 2009;**41**(11):1264-76.
[7] Lemaitre J. *A Course on Damage Mechanics*. Berlin: Springer; 1992.
[8] Gurson AL. Continuum Theory of Ductile Rupture by Void Nucleation and Growth: Part I—Yield Criteria and Flow Rules for Porous Ductile Media. *Journal of Engineering Materials and Technology*. 1977;**99**(1):2-15.
[9] Isik K, Gerstein G, Schneider T, Schulte R, Rosenbusch D, Clausmeyer T, et al. Investigations of ductile damage during the process chains of toothed functional components manufactured by sheet-bulk metal forming. *Production Engineering*. 2016;**10**(1):5-15.
[10] Sieczkarek P, Kwiatkowski L, Ben Khalifa N, Tekkaya AE. Novel Five-Axis Forming Press for the Incremental Sheet-Bulk Metal Forming. *Key Engineering Materials*. 2013;**554-557**:1478-83.
[11] Sieczkarek P, Wernicke S, Weddeling C, Martins PA, Tekkaya AE, editors. *Local forming of gears by indentation of sheets*. Proceedings of the Institution of Mechanical Engineers, Part B: Journal of Engineering Manufacture.
[12] Isik K, Gerstein G, Clausmeyer T, Nürnberger F, Tekkaya AE, Maier HJ. Evaluation of Void Nucleation and Development during Plastic Deformation of Dual-Phase Steel DP600. *steel research international*. 2016;**87**(12):1583-91.
[13] Tvergaard V, Needleman A. Analysis of the Cup-Cone Fracture in a Round Tensile Bar. *Acta Metall Mater*. 1984;**32**(1):157-69.
[14] Nahshon K, Hutchinson JW. Modification of the Gurson Model for shear failure. *European Journal of Mechanics - A/Solids*. 2008;**27**(1):1-17.
[15] Isik K, Gerstein G, Gutknecht F, Clausmeyer T, Nürnberger F, Maier HJ, et al. Investigations of ductile damage in DP600 and DC04 deep drawing steel sheets during punching. *Procedia Structural Integrity*. 2016;**2**:673-80.